Structural and electrochemical properties of carbon-coated Li$_4$Ti$_5$O$_{12}$ anodic material obtained using chitosan for potential lithium ion rechargeable battery applications

Eun Hyuk Chung[a], Hyun Ju Han[b], F. Nawaz Khan[c], Tae Eun Hong[a], Hyun Gyu Kim[a], Jong-Seong Bae[a], Ok-Sang Jung[b], Hee Jung[d], Jong Pil Kim[a], Jong Sung Jin[a] and Euh Duck Jeong[a,*]

[a]*Division of High-Technology Materials Research, Korea Basic Science Institute, Busan 618-230, Korea*
[b]*Department of Chemistry, Pusan National University, Busan 627-706, Korea*
[c]*Organic and Medicinal Chemistry Research Laboratory, School of Advanced Sciences, VIT University, Vellore, Tamil Nadu 632-014, India*
[d]*Small Enterprise Development Agency, Daejeon 302-829, Korea*

The sol-gel methodology is employed for the preparation of chitosan added carbon-coated Li$_4$Ti$_5$O$_{12}$ anode material with improved electrochemical properties for the lithium ion battery applications. The XRD shows that the coating of carbon does not influence the formation of Li$_4$Ti$_5$O$_{12}$ and the carbon coating on the surface of lithium titanate, Li$_4$Ti$_5$O$_{12}$ are confirmed by XPS, TEM and Nano-SIMS. A charge/discharge test performed at 0.1 ºC and 0.2 ºC hour rate, shows that the rate capability and cycle performance are improved due of the chitosan addition which produced carbon coating on the surface of the Li$_4$Ti$_5$O$_{12}$ material. Similarly the chitosan added carbon-coated Li$_4$Ti$_5$O$_{12}$ show higher specific capacity 142 mAhg^{-1} with superior cycling properties against uncoated Li$_4$Ti$_5$O$_{12}$ material 132 mAhg^{-1}. Also the carbon coating improves the overall electrochemical properties including discharge capacity, cyclability and rate capability against pure Li$_4$Ti$_5$O$_{12}$.

Key words: Lithium-ion batteries, Lithium titanate, Sol-gel reaction, Carbon-coating, Electrochemical properties, Nano secondary ion mass spectrometry.

Intrduction

The rechargeable lithium-ion batteries nowadays have been popular, due to their potential use in portable electronic devices and in other fields, including automotive applications [1-5]. In search of highly improved cathodes for the lithium ion battery applications, recently carbon coated LiFePO$_4$ [6], Al$_2$O$_3$ and AlF$_3$ coated LiFePO$_4$ [7], chitosan added LiFePO$_4$ [8], LiCoO$_2$ [9, 10] cathodes with improved electrochemical properties has been reported by us. In our continued interest on rechargeable lithium ion batteries, the current research is directed towards the search of efficient anode materials as new electrode materials exhibiting high charge/discharge current rates are urgently requested.

The carbon is the most exploited anode in the commercial Li-ion batteries; however, chemical and electrochemical concerns associated with carbon make it less preferred for long term and high power battery applications. Lithium titanate anode provides a number of significant advantages over its carbon counterpart, for eg. the lithium titanate based batteries can be fully charged within 10 minutes, have exceptional cycle,

'zero-strain' effect and the flat Li insertion voltage, features flat operation voltage of 1.5 V versus Li+/Li and are very promising for large number of applications. Similarly, the lithium titanate operates at a higher voltage at which lithium ions are stable with respect to the electrolyte and hence the solid electrolyte interface, overheating problem is eliminated. Also possess number of different applications such as PHEV, EV, power tools, peak saving, and power grid [11-20].

The lithium titanate anode possess high theoretical capacity, high cyclability and high rate ability to charge and discharge, a very safe, cheap indeed have the limitation of electronic conductivity. It is envisioned that the drawback of lithium titanate anode having smaller electronic conductivity can be eliminated by decreasing its particle size (which reduces lithium diffusion path and enlarges interfacial surface) [21-23] or covering particle surface with carbon (conductive surface coating), [24-29] doping with metals (which improves electrode stability by rising electronic conductivity and deflating anode polarization), [30-37].

There are several methods including solid state reaction, sol-gel, water burning; gel-emulsion process, hybrid microwave synthesis, the structure and the electrochemical performance of lithium titanate depend on the synthesis method. However through all these methods nanosized particle could not be obtained; the

*Corresponding author:
Tel : +82-51-974-6100
Fax: +82-51-974-6116
E-mail: edjeong@kbsi.re.kr

transition from micron to nanosized electrode material would improve the performance of lithium-ion batteries. The introduction of nanosized $Li_4Ti_5O_{12}$ (n-LTO) anodes for Li-ion batteries has opened new avenues to the cycle-life in Li-ion batteries [38-41].

Here in we report the chitosan added carbon-coated $Li_4Ti_5O_{12}$ with improved electronic conductivity prepared by adding chitosan to the precursors during sol gel methodology. The various physical and electrochemical parameters are discussed in detail. To elucidate significantly the characteristics of the chitosan added carbon-coated $Li_4Ti_5O_{12}$ powders, the thermal analysis, XRD, XPS, SEM, TEM and Nano-SIMS have been employed.

The NanoSIMS which couples a high transmission, high mass resolution mass spectrometer represents the state-of-the-art for in situ microanalysis by secondary ion mass spectrometry [42-44]. The primary ion beam (down to < 50 nm for Cs^+ primary ions and 150 nm for O- primary ions) can be scanned across the sample to produce quantitative secondary ion images. The NanoSIMS provides a novel new approach to the study of the isotope and trace element distributions and an unprecedented ability for correlated analyses of morphological, structural, chemical and isotopic characteristics with nanometer resolution using SEM, TEM and NanoSIMS. In combination with other analytical such as optical microscopy, AFM, SEM and EPMA it is possible to carry out multi-technique analysis and complement the chemical maps acquired by the NanoSIMS in a range of projects in the analysis of metallic and polymeric materials, cancer cells, cancer tissue, trace elements in cereal grains and metal hyper accumulator plants [45-50].

In this study, high resolution secondary ion mass spectrometry (NanoSIMS) analysis has been performed on $Li_4Ti_5O_{12}$ materials obtained from chitosan added precursors. Elemental maps are obtained which revealed the high concentrations of carbon throughout the surface of the $Li_4Ti_5O_{12}$ materials. The superior spatial resolution (better than 50 nm) and ultrahigh chemical sensitivity (< 200 atom detection limit) of the NanoSIMS technique provided carbon abundances which were used to produce maps of the tiniest particles, revealing a more detailed image of carbon distribution in chitosan added carbon-coated $Li_4Ti_5O_{12}$ material.

In addition, the electrochemical properties of the electrodes including charge-discharge experiment to compare the efficiency of bare $Li_4Ti_5O_{12}$ and chitosan added carbon-coated $Li_4Ti_5O_{12}$ materials have been employed.

Experimental

The $Li_4Ti_5O_{12}$ based anode materials for lithium ion battery were prepared using sol-gel method. The $Li_4Ti_5O_{12}$ precursor required for the present study was prepared by mixing lithium acetate (LiAc·2H₂O, Aldrich, 98%) and titanium isopropoxide ($Ti(OC_4H_9)_3$, Aldrich,

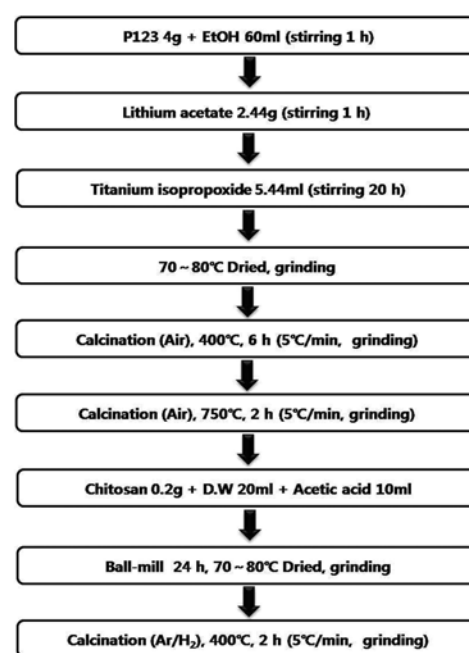**Fig. 1.** A preparation diagram of the $Li_4Ti_5O_{12}$ powder.

97%) thoroughly. Similarly the carbon coated $Li_4Ti_5O_{12}$ precursor, was prepared by adding chitosan, ($C_{12}H_{24}N_2O_9$, Aldrich, viscosity 20,000 cps] in acetic acid to the above mixture. Both the materials $Li_4Ti_5O_{12}$ precursor and carbon coated $Li_4Ti_5O_{12}$ precursor were analyzed using thermogravimetric analyzer (TGA, TA Instruments SDT Q 600).

The $Li_4Ti_5O_{12}$ precursor was initially calcined at 400 °C for 6 hour and then calcined again at 750 °C for 2 hours. All calcinations were done under air. The chitosan added carbon-coated $Li_4Ti_5O_{12}$ was also calcinated twice as described above. Then the chitosan added carbon-coated $Li_4Ti_5O_{12}$ was ball milled for 24 hours and calcined again at 400 °C for 2 hours in Ar/H_2.

Fig. 1 displays the preparation diagram of the $Li_4Ti_5O_{12}$ precursor. The synthesized materials were characterized using the conventional X-ray diffractometer (XRD, Rigaku D-2400), X-ray photoelectron spectroscopy (XPS, Escalab 250), scanning electron microscope (SEM, Hitachi S-4200), transmission electron microscopy (TEM, JEM 2011) and Nano-secondary ion mass spectroscopy (Nano-SIMS, CAMECA).

The $Li_4Ti_5O_{12}$ electrodes required for the study was obtained from the synthesized $Li_4Ti_5O_{12}$ powders, Super P. carbon black as a conductive material, and N-methyl-2-pyrrolidone (NMP) solution containing poly vinylidene difluoride (PVDF, Aldrich, average MW: 534,000) as a binder. The electrochemical properties of the $Li_4Ti_5O_{12}$ electrodes were investigated by mixing 85 wt% $Li_4Ti_5O_{12}$, 10 wt% conducting compound as a conductive material, and 5 wt% PVDF binder to a NMP solution. The kneaded slurry with an adequate viscosity was coated on a copper foils. The coated sheets were dried under air 100 °C for 1 hour and pressed.

The electrodes were in a vacuum dried at 24 hours.

Coin-type cell composed $Li_4Ti_5O_{12}$ anode, lithium metal ribbon, and polyethylene (PE) separator were used in a supporting electrolyte. The ethylene carbonate (EC, Mitsubishi Petrochemical Co., battery grade), diethyl carbonate (DEC, Mitsubishi Petrochemical Co., battery grade solution [EC/DEC, 1 : 1 with the volume ratio] containing 1 M $LiPF_6$ (Aldrich) were used as supporting electrolytes. The charge/discharge experiment was carried out galvanostatically by using the battery testing instrument (TOSCAT-3000U, Toyo). The galvanostatic charge and discharge experiments were conducted with the cutoff voltages set to be 1.0 V and 2.5 V for charge and discharge, respectively.

Results and Discussion

Fig. 1 displays the preparation diagram of the chitosan added carbon-coated $Li_4Ti_5O_{12}$ precursor.

The oxidation resistance of chitosan added carbon-coated $Li_4Ti_5O_{12}$ was determined by thermogravimetric analysis (TGA) in Fig. 2. The TGA profiles of the uncoated and chitosan added carbon-coated $Li_4Ti_5O_{12}$ revealed that the chitosan added carbon-coated $Li_4Ti_5O_{12}$ showed the main weight loss around 300 ~ 400 °C due to oxidation of carbon, releasing CO_2 gas (which manifested in an exothermic peak), and water removal (below 300 °C). Significant changes are observed
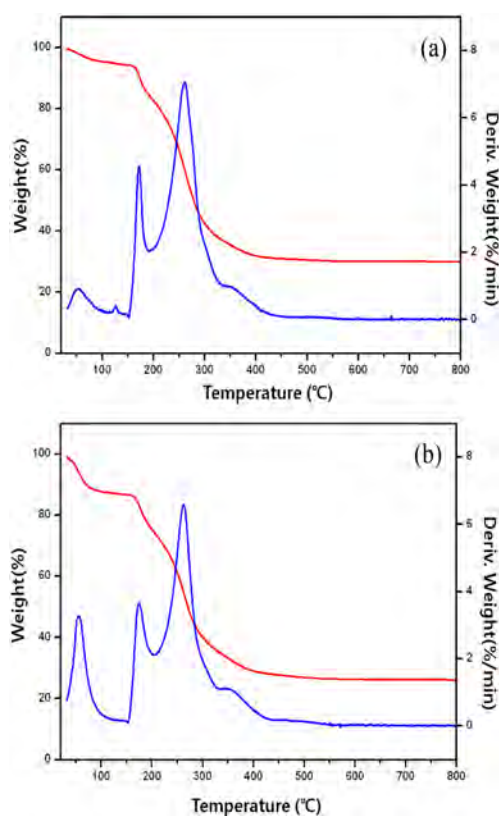
around from 200 °C to 300 °C and these two points were chosen as the calcinations temperatures of the $Li_4Ti_5O_{12}$ precursors. The comparative analysis of bare and chitosan added carbon-coated $Li_4Ti_5O_{12}$ nanoparticles revealed that the latter possess better oxidation resistance than the bare $Li_4Ti_5O_{12}$.

The X-ray diffraction patterns of the samples are shown in Fig. 3, it can be observed that the main phases of all investigated samples are $Li_4Ti_5O_{12}$, which suggests that the addition of chitosan in the precursor does not influence the formation of $Li_4Ti_5O_{12}$ during heat-treatment.

The XRD pattern showed no good crystallization at 650 °C calcination. The calcinations at 750 °C and 850 °C for 2 hours gave similar pattern. Furthermore, Fig. 3 showed weak peaks at characteristic 2-theha
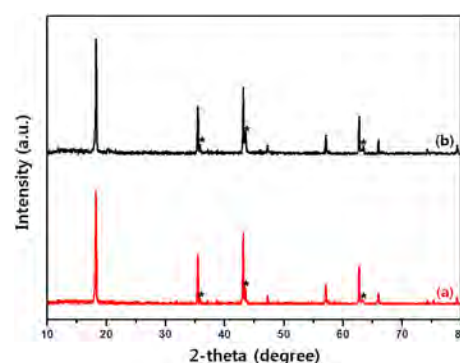

Fig. 3. XRD patterns for (a) the pure-$Li_4Ti_5O_{12}$ and (b) chitosan added carbon-coated $Li_4Ti_5O_{12}$ powder which are calcined at 750 °C. Small *peaks were TiO_2 powder.

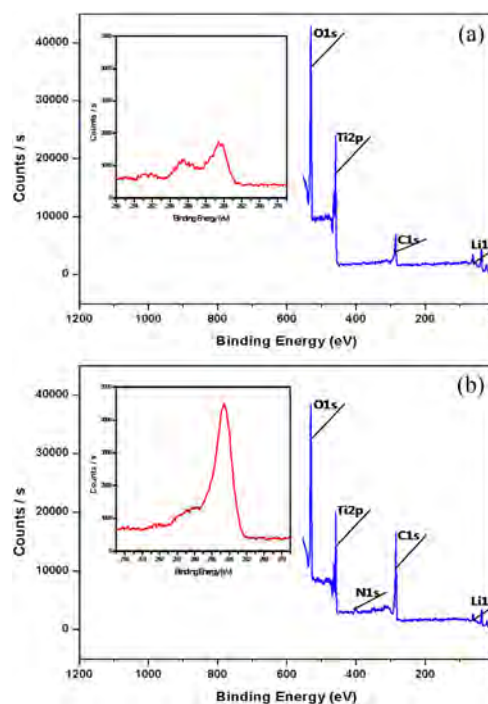**Fig. 2.** TG/DTA curves recorded for (a) the pure-$Li_4Ti_5O_{12}$ and (b) chitosan added carbon-coated $Li_4Ti_5O_{12}$ powder.

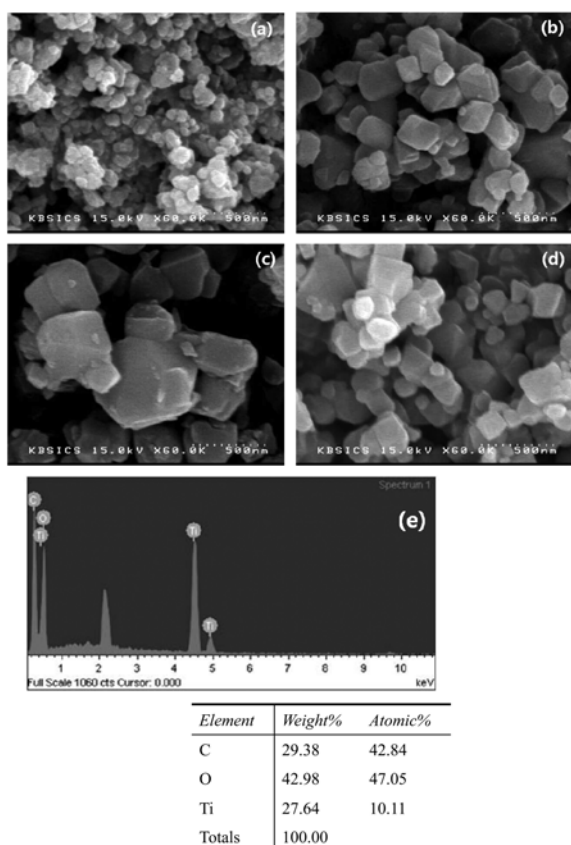**Fig. 4.** Wide scan XPS spectra for (a) pure-$Li_4Ti_5O_{12}$, (b) chitosan added carbon-coated $Li_4Ti_5O_{12}$.

Fig. 5. SEM images of chitosan added carbon-coated $Li_4Ti_5O_{12}$ after the second calcinations at (a) 650 °C, (b) 750 °C, (c) 850 °C, (d) pure $Li_4Ti_5O_{12}$ at 750 °C and (e) SEM EDS data chitosan added carbon-coated $Li_4Ti_5O_{12}$.

Element	Weight%	Atomic%
C	29.38	42.84
O	42.98	47.05
Ti	27.64	10.11
Totals	100.00	

Fig. 6. TEM images of the synthesized chitosan added carbon-coated $Li_4Ti_5O_{12}$ powders.

Fig. 7. Elemental image mapping analysis by Nano-SIMS for (a) pure- $Li_4Ti_5O_{12}$ and (b) chitosan added carbon-coated $Li_4Ti_5O_{12}$.

indicating that the Li-Ti-O phase may contain smaller amout of rutile phase TiO_2 powder.

Fig. 4 shows wide scan XPS spectra for pure-$Li_4Ti_5O_{12}$ (a), chitosan added carbon-coated $Li_4Ti_5O_{12}$ (b). All elements such as Li, Ti, C and O are observed. The carbon intensities were increased when chitosan is added $Li_4Ti_5O_{12}$. Since XPS spectra were taken in vacuum without etching the surface of the samples, the carbon peak appeared in $Li_4Ti_5O_{12}$ power (a) is considered due to the residual carbon from the atmosphere or the precipitates in synthesis process.

Fig. 5 depicts the SEM images of the carbon-coated $Li_4Ti_5O_{12}$ material obtained after calcinations at different temperatures. It can be seen that the sizes of $Li_4Ti_5O_{12}$ particles are 100 nm at 750 °C and are agglomerated. It can be observed that the particles of $Li_4Ti_5O_{12}$ have relatively less agglomerations at 650 °C while the particles of $Li_4Ti_5O_{12}$ form larger agglomeration at 850 °C. Furthermore, as is shown in the close up SEM images the particle surface of $Li_4Ti_5O_{12}$ is smooth at higher temperature calcinations, whereas the $Li_4Ti_5O_{12}$ calcined at low temperatures have a rougher surface, which should be ascribed to particle growth during heat-treatment. The SEM EDX image gives the composition of the chitosan added carbon-coated $Li_4Ti_5O_{12}$ (Fig.
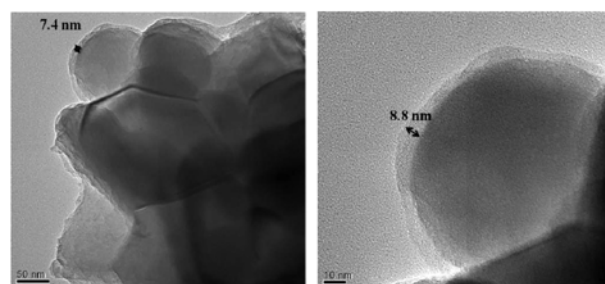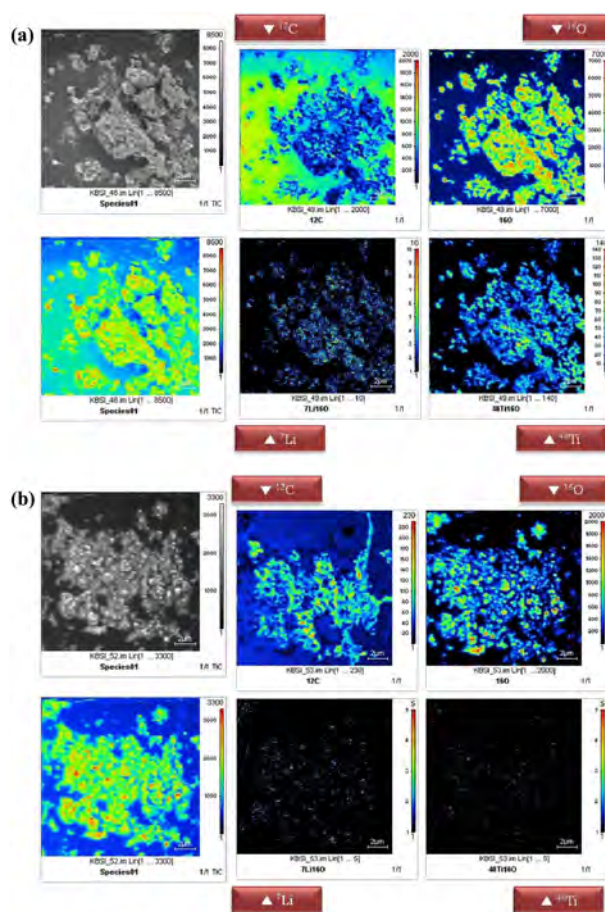
5(e)), the SEM image of pure $Li_4Ti_5O_{12}$ (Fig. 5(d)).

In order to investigate the carbon coating on the surface of $Li_4Ti_5O_{12}$ powder, the TEM measurements were carried out. The TEM images Fig. 6, showed that chitosan added carbon-coated $Li_4Ti_5O_{12}$ powders at 400 °C for 2 hours in Ar/H₂. It is clear that carbon is deposited on the surface of the chitosan added carbon-coated $Li_4Ti_5O_{12}$ powders in a form of a nanometer-thick layer of carbon. The thickness of carbon layer is measured to be about 7.4 ~ 8.8 nm. The electronic conductivity study of the synthesized material indicated that they got influenced by the carbon layer exists on the surface of $Li_4Ti_5O_{12}$ as discussed latter in this article.

Fig. 9. The specific capacity electrode materials at discharge rate of 0.2 C with the number of cycles. The squares represent pure $Li_4Ti_5O_{12}$ (a), and circles represent chitosan added carbon-coated $Li_4Ti_5O_{12}$ (b). In both cases, the charge/discharge rates were (a) 0.1 C, (b) 0.2 C, (c) 0.5 C, (d) 1 C, (e) 2 C.
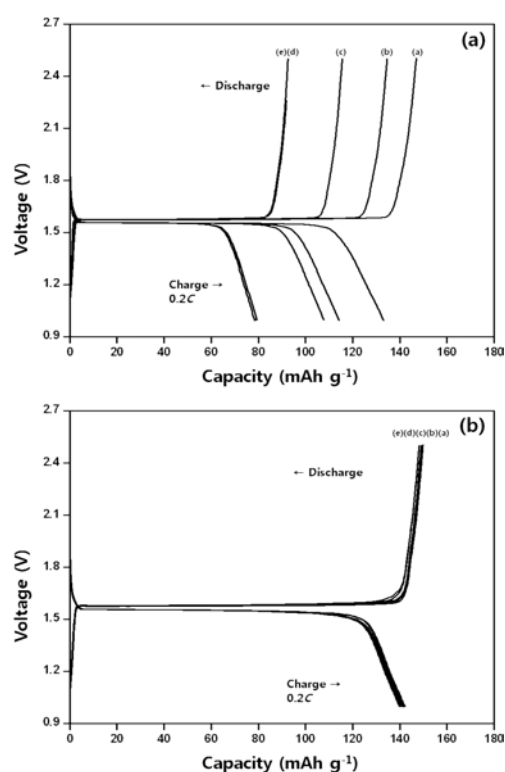
Fig. 8. The discharge voltage profiles for the electrodes as a function of the specific capacity for (a) pure- $Li_4Ti_5O_{12}$ and (b) chitosan added carbon-coated $Li_4Ti_5O_{12}$. In both cases, the charge/discharge rates were (a) 0.1 C, (b) 0.2 C, (c) 0.5 C, (d) 1 C, (e) 2 C.

The Fig. 7 represents the atom image mapping analysis by Nano-SIMS of the uncoated and chitosan added carbon-coated $Li_4Ti_5O_{12}$ materials. By comparing the images, it can be observed that the surface of the latter materials is totally and uniformly covered by the nanosized carbon layer. Consequently, Li, Ti and O atoms mapping images are a little observed.

The Fig. 8 shows the charge–discharge curves of the $Li_4Ti_5O_{12}$ and chitosan added carbon-coated $Li_4Ti_5O_{12}$ electrodes at different rates from 0.1 to 2.0 C viz. 0.1, 0.2, 0.5, 1 and 2 C. There, it can be seen that both the materials have similar graph–which indicates that the addition of chitosan did not affect the electrochemical reaction process of $Li_4Ti_5O_{12}$. When charge-discharge rate increases from 0.1 to 0.2 C the capacity decreases quickly from 133.1 mAhg^{-1} to 130 mAhg^{-1} which is 97.67% rate capacity for the pure $Li_4Ti_5O_{12}$ material, similarly from 142 mAhg^{-1} to 141.8 mAhg^{-1} which is 99.85% rate capacity for the chitosan added carbon-coated $Li_4Ti_5O_{12}$ material which indicates that the improved electrochemical properties of the latter material. It is obvious that the discharge capacity of chitosan added carbon-coated $Li_4Ti_5O_{12}$ had better performance than that of $Li_4Ti_5O_{12}$ by delivering higher charge and discharge capacity at the same current densities of 0.1, 0.2 C etc.

At the rates from 0.1 to 0.5 C, the variation of discharge capacity and discharge plateau potential are very small. The discharge potential is near 1.55 V
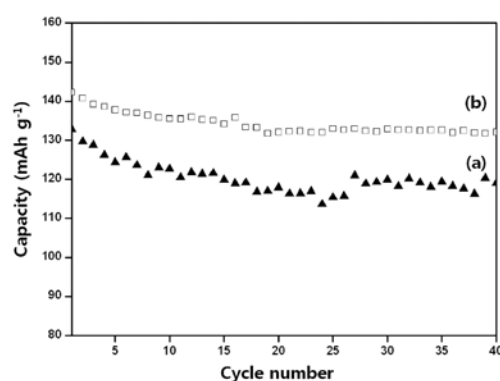
(reversible redox potential of $Li_4Ti_5O_{12}$ material). Furthermore, the margins between the charge and discharge plateau potentials of chitosan added carbon-coated $Li_4Ti_5O_{12}$ are obviously smaller than in the case of $Li_4Ti_5O_{12}$, and the has the smallest margin at 0.1 C, which means that the polarization of chitosan added carbon-coated $Li_4Ti_5O_{12}$ are lower than that of $Li_4Ti_5O_{12}$, and the chitosan added carbon-coated $Li_4Ti_5O_{12}$ has the smallest polarization at 0.1 C. The voltage profile of the chitosan added carbon-coated $Li_4Ti_5O_{12}$ showed smoothly sloped shape compared to bare $Li_4Ti_5O_{12}$.

The Fig. 9 shows the cycling behavior of our chitosan added carbon-coated lithium titanate anode material at 0.2 C operated between 1.0 and 2.5 V. As shown in Fig. 9, the discharge capacity gradually decreased with the increased cycle for all the samples. The initial reversible specific capacity of the bare $Li_4Ti_5O_{12}$ sample is 132 mAhg^{-1} and after 40 cycles its value remains at 119 mAhg^{-1} in comparison to 142 mAhg^{-1} and 132 mAhg^{-1} respectively for the carbon coated $Li_4Ti_5O_{12}$ material. The capacity fading was almost concentrated in the first 10 cycles in the former, whereas the cell cyclability in 40 cycles clearly demonstrates the absence of negligible capacity fading in the chitosan added carbon-coated $Li_4Ti_5O_{12}$ material, similarly, the chitosan added carbon- coated $Li_4Ti_5O_{12}$ manifested a higher reversible capacity than the $Li_4Ti_5O_{12}$ sample, especially at higher cycles indicating the carbon coated material exhibits the better rate capability. The chitosan added carbon-coated $Li_4Ti_5O_{12}$ nanoparticles show superior cycling properties compared with the uncoated ones as in the latter, most of the capacity was lost after 20 cycles. Columbic charge efficiency is excellent with efficient and rapid insertion and extraction of lithium, independent of rate. A rate capability of 142 mAhg^{-1} at 0.1 C demonstrates its potential toward its uses in moderate to high rate applications, while capacity at 0.2 C rates is 141.8 mAhg^{-1}.

Conclusions

The chitosan added carbon-coated $Li_4Ti_5O_{12}$ was synthesized and its electrochemical characteristics were investigated in the present study. For comparison, $Li_4Ti_5O_{12}$ were also investigated. The results show that chitosan added carbon-coated $Li_4Ti_5O_{12}$ has better electrochemical performance due to the conductive second carbon phase which uniformly coated on the surface of $Li_4Ti_5O_{12}$ particles and could improve the rate capability and cycling stability of $Li_4Ti_5O_{12}$ and are favorable to the electrons transfer thereby improving electronic conductivity. These characteristics indicate that chitosan added carbon-coated $Li_4Ti_5O_{12}$ is advantageous as a good candidate as negative electrode for solid state lithium ion batteries and super capacitor with safety, long life period and reliability. Phase purity, high crystallinity and small particles with narrow size distribution are always required.

Acknowledgments

References

1. B. Scrosati, Nature 373 (1995) 557-558.
2. J.M. Tarascon, M. Armand, Nature 414 (2001) 359-367.
3. D. Guyomard in: T. Osaka, M. Datta (Eds.), Energy Storage Systems for Electronics New Trends in Electrochemical Technology, Gordon & Breach Science Publishers (2000) 253-350.
4. M. Wakihara, O. Yamamoto (Eds.), Lithium Ion Batteries, Fundamentals and Performance, Kodansha Ltd., Tokyo (1998).
5. P.G. Bruce, B. Scrosti, J.M. Tarascon, Angew. Chem. Int. Ed. 47 (2008) 2930-2946.
6. E.D. Jeong, H.J. Kim, C.W. Ahn, M.G. Ha, T.E. Hong, H.G. Kim, J.S. Jin, J.S. Bae, K.S. Hong, Y.S. Kim, H.J. Kim, C.H. Doh, H.S. Yang, Journal of Nanoscience and Nanotechnology 9 (2009) 4467-4471.
7. C.W. Ahn, M.G. Ha, K.S. Hong, D.J. Lee, C.H. Doh, K.Y. Doh, J.M. Na, B.H. Song, H.M. Jeon, Y.G. Cho, H.S. Yang, E.D. Jeong, Defect and Diffusion Forum 297-301 (2010) 906-911.
8. K.S. Hong, S.M. Yu, M.G. Ha, C.W. Ahn, T.E. Hong, J.S. Jin, H.G. Kim, E.D. Jeong, Y.S. Kim, H.J. Kim, C.H. Doh, H.S. Yang, H. Jung, Bull. Korean Chem. Soc. 30 (2009) 1719-1723.
9. P.J. Cho, E.D. Jeong, Y.B. Shim, Bull. Korean Chem. Soc. 19 (1998) 39-44.
10. E.D. Jeong, M.S. Won, Y.B. Shim, J. Power Sources 70 (1998) 70-77.
11. K.M. Colbow, J.R. Dahn, R.R. Haering, J. Power Sources 26 (1989) 397-402.
12. K. Zaghib, M. Armand, M. Gauthier, J. Electrochem. Soc. 145 (1998) 3135-3140.
13. T. Ohzuku, Y. Iwakoshi, K. Sawai, J. Electrochem. Soc. 140 (1993) 2490-2498.
14. K. Zaghib, M. Simoneau, M. Armand, M. Gauthier, J. Power Sources 81-82 (1999) 300-305.
15. A. Guerfi, S. Sevigny, M. Lagace, P. Hovington, K. Kinoshita, K. Zaghib, J. Power Sources 119-121 (2003) 88-94.
16. S. Scharner, W. Weppner, P. Schmid-Beurmann, J. Electrochem. Soc. 146 (1999) 857-861.
17. M.M. Thackeray, P.J. Johnson, L.A. de Picciott, P.G. Bruce, J.B. Goodenough, Mater. Res. Bull. 19 (1984) 179-187.
18. T. Ohzuku, A. Ueda, N. Yamamoto, J. Electrochem. Soc. 142 (1995) 1431-1435.
19. D. Peramunage, K.M. Abraham, J. Electrochem. Soc. 145 (1998) 2609-2615.
20. Q. Wang, P. Pechy, S.M. Zakeeruddin, I. Exnar, M. Grätzel, J. Power Sources, 146 (2005) 813-816.
21. A. Guerfi, S. Sévigny, M. Lagacé, P. Hovington, K. Kinoshita, K. Zaghib, J. Power Sources 119-121 (2003) 88-94.
22. K.N. Jung, S.I. Pyun, S.W. Kim, J. Power Sources 119-121 (2003) 637-643.
23. E.D. Jeong, M.G. Ha, J.S. Bae, K.S. Hong, J. Anal. Sci. & Tech. 2 (2011) 7-12.
24. S.H. Huang, Z.Y. Wen, J.C. Zhang, Z.H. Gu, X.H. Xu, Solid State Ionics 177 (2006) 851-855.
25. R. Dominko, M. Gaberscek, U. Bele, D. Mihailovic, J. Jamnik, J. European Ceramic Soc. 27 (2007) 909-913.
26. H. Liu, Y. Feng, K. Wang, J.Y. Xie, J. Physics and Chemistry of Solids 69 (2008) 2037-2040.
27. J.J. Huang, Z.Y. Jiang, Electrochimica Acta 53 (2008) 7756-7759.
28. L.X. Yang, L.J. Gao, J. Alloys Compounds 485 (2009) 93-97.
29. J. Wolfenstine, U. Lee, J.L. Allen, J. Power Sources 154 (2006) 287-289.
30. D.T. Liu, C.Y. Quyang, J. Shu, J. Jiang, Z.X. Wang, L.Q. Chen, Physics Status Solid B 243 (2006) 1835-1841.
31. Y.J. Hao, Q.Y. Lai, J.Z. Lu, X.Y. Ji, Ionics 13 (2007) 369-373.
32. P. Kubiak, A. Garcia, M. Womes, L. Aldon, J. Olivier-Fourcade, P.E. Lippens, J.C. Jumas J. Power Sources 119-121 (2003) 626-630.
33. S.H. Huang, Z.Y. Wen, Z.H. Gu, X.J. Zhu, Electrochimica Acta 50 (2005) 4057-4062.
34. S.H. Huang, Z.Y. Wen, X.J. Zhu, Z.X. Lin, J. Power Sources 165 (2007) 408-412.
35. H.Y. Yu, X.F. Zhang, A.F. Albout, X.D. Yan, X.M. Pan, H.M. Xie, R.S. Wang, Electrochimica Acta 53 (2008) 4200-4204.
36. T. Tabuchi, H. Yasuda, M. Yamachi, J. Power Sources 162 (2006) 813-817.
37. J. Wolfenstine, J.L. Allen, J. Power Sources 180 (2008) 582-585.
38. L. Kavan, J. Procházka, T.M. Spitler, M. Kalbáè, M. Zukalová, T. Drezen, M. Grätzel, J. Electrochem. Soc. 150 (2003) A1000-A1007.
39. G.G. Amatucci, F. Badway, A.D. Pasquier, T. Zheng, J. Electrochem. Soc. 148 (2001) A930-A939.
40. G.X. Wang, D.H. Bradhurst, S.X. Dou, H.K. Liu J. Power Sources 83 (1999) 156-161.
41. G. Amatucci, A.D. Pasquier, A. Blyr, T. Zheng, J.M. Tarascon, Electrochimica Acta 45 (1999) 255-271.
42. J.W. Moreau, P.K. Weber, M.C. Martin, B. Gilbert, I.D. Hutcheon, J.F. Banfield, Science 316 (2007) 1600-1603.
43. N. Musat, H. Halm, B. Winterholler, P. Hoppe, S. Peduzzi, F. Hillion, F. Horreard, R. Amann, B.B. Jørgensen, M.M.M. Kuypers, PNAS 105 (2008) 17861-17866.
44. C.J. Simensen, O. Nielsen, F. Hillion, J. Voje, Metallurgical and Materials Transactions A 38 (2007) 1448-1451.
45. K.L. Moore, M. Schröder, E. Lombi, F.J. Zhao, S.P. McGrath, M.J. Hawkesford, P.R. Shewry, C.R.M. Grovenor, New

Phytologist 185 (2010) 434-445.

46. K.E. Smart, J.A.C. Smith, M.R. Kilburn, B.G.H. Martin, C. Hawes, C.R.M. Grovenor, The Plant Journal 63 (2010) 870-879.

47. S. Lozano-Perez, M. Schröder, T. Yamada, T. Terachi, C.A. English, C.R.M. Grovenor, Appl. Surf. Sci. 255 (2008) 1541-1543.

48. S. Lozano-Perez, M.R. Kilburn, T. Yamada, T. Terachi, C.A. English, C.R.M. Grovenor, J. Nucl. Mater. 374 (2008) 61-68.

49. S. Ahmed, J.M. Titchmarsh, M.R. Kilburn, C.R.M. Grovenor, Appl. Surf. Sci. 252 (2006) 7062-7065.

50. C. Dark, M.R. Kilburn, G. Hammerl, C. Schneider, J. Mannhart, C.R.M. Grovenor, J. Phys. Conf. Ser. 43 (2006) 272-276.